

**Chromate immobilization in groundwater and soil  
using Iron-Manganese binary metal oxide nanoparticles**

by

Mengwei Yao

A thesis submitted to the Graduate Faculty of  
Auburn University  
in partial fulfillment of the  
requirements for the Degree of  
Master of Environmental Science

Auburn, Alabama  
December 12, 2015

Key words: chromate, groundwater, removal, immobilization, nanoparticles

Copyright 2015 by Mengwei yao

Approved by

Dongye Zhao, Chair, Huff Professor of Civil Engineering  
Mark O. Barnett, Malcolm Pirnie Professor of Civil Engineering  
Clifford R. Lange, Associate Professor of Civil Engineering

## Abstract

Fe-Mn (iron – manganese binary oxide) nanoparticle were synthesized and test for the Cr(VI) immobilization in soil and groundwater. Water soluble starch and carboxymethyl cellulose (CMC) were applied to stabilize the nanoparticles. All three particles exhibited a fast adsorption kinetic while only bare and starch stabilized Fe-Mn showed a high removal efficiency. The Langmuir adsorption capacity of bare, starch and CMC stabilized nanoparticle were 59 mg/g, 54mg/g, and 2 mg/g, respectively. The high removal efficiency was observed at pH rang of 3-6. Competing ions and humic acid test indicated the starch coating could shield the core Fe-Mn from effect by sulfate and phosphate, the removal efficiency of starch Fe-Mn remain greater than 95% in the presence of 5 mg/L humic acid. Column tests show that after 4 pore volume about 20% of starch stabilized Fe-Mn was retained in soil, which indicated the deliverable of starch stabilized particles. Treatment with starch stabilized Fe-Mn could reduce up to 85% of soluble Cr(VI) leaching in soil compare to DI water.

## Acknowledgments

I would never have been able to approach to a master degree without the guidance from my committee members, support from my family, and help from my friends.

First of all, I would like to acknowledge my thesis advisor Dr. Dongye Zhao for his support, guidance, inspiration, motivation, and friendship. He identified important aspects of my research initially, consistently provided me with an excellent atmosphere for experiments, directed me to translate them into my master thesis, which inspired and enriched my growth as a student and an engineer. I have learned a lot from his expertise of environmental engineering and chemistry.

I gratefully thank Dr. Mark O. Barnett, Dr. Clifford Lange for their services on my master committee, inspiring comments and thoughtful criticism. It is my honor and pleasure working with them. Without the help and support of my labmates, this thesis would not have been possible. I'd especially like to thank Jinling Zhuang for the experimental and analytical assistance. I would also like to thank Dr. Wen Liu, Dr. Xiao Zhao, Dr. Bing Han, Xue Wang, Zhengqing Cai, Shuting Tian, Haodong Ji, Zhen Huang, as well as other members of environmental engineering program here at Auburn University for their research advices and for creating a supportive environment.

Finally, I'd like to thank my parents and sister, for their understanding, forgiveness, encouragements and love. Thanks are also due to other family members for their support during these precious years.

## Table of Contents

Abstract.....	ii
Acknowledgments.....	iii
List of Tables .....	v
List of Figures .....	vi
List of Abbreviations .....	viii
<b>Chapter 1. Introduction.....</b>	<b>1</b>
<b>Chapter 2 Chromate immobilization in Soil and Groundwater using stabilized Fe-Mn nanoparticles .....</b>	<b>3</b>
2.1. Introduction.....	3
2.2. Material and methods.....	4
<b>Chapter 3 Result and discussion.....</b>	<b>10</b>
3.1. Characterization of adsorbent .....	10
3.2 Stabilizer dosage effect on Cr(VI) removal .....	17
3.3 Kinetic of Cr(VI) removal by Fe-Mn nanoparticle .....	19
3.4. Effect of pH and competing ions .....	23
3.6 Effect of humic acid.....	27
3.7 Cr(VI) immobilization in soil: column tests .....	29
3.5 Conclusions.....	32
References.....	34

## List of Tables

Table 1 Characteristic of Loamy sandy soil used in experiment .....	5
Table 2 Calculation of pseudo second order model.....	19
Table 3 Langmuir model parameter for bare, starch and CMC Fe-Mn.....	21

## List of Figures

Figure 1 FT-IR spectra of bare and starch stabilized Fe-Mn nanoparticles before and after .....	11
Figure 2 XPS analysis of bare and stabilized Fe-Mn before and after adsorption of Cr(VI). .....	14
Figure 3 Zeta potential of bare, starch or CMC stabilized Fe-Mn as a function of pH. Initial condition: Cr(VI) = 5 mg/L, starch = 0.19 wt. %, CMC = 0.16 wt. %, Fe = 0.2 g/L, Mn = 0.07 g/L.....	16
Figure 4 Chromate removal efficiency as a function of various starch concentration. Initial condition: Cr(VI) = 10 mg/L, pH = 6 ±0.1, Fe = 0.2 g/L, Mn = 0.07 g/L.(All samples were made in duplicated) .....	18
Figure 5 Kinetic of Cr(VI) removal with bare or stabilized Fe-Mn nanoparticles. C0 and C represent the initial concentration and concentration at time t of Cr(VI), respectively. Initial Cr(VI) = 5 mg/L, nanoparticles = 0.27 g/L (Fe =0.2 g/L; Mn = 0.07 g/L), starch = 0.19 wt.%, CMC = 0.16 wt. %, pH = 6 ±0.1. Symbols : Experimental data; Lines : Pseudo second order model. All data are duplicated, errors indicate the standard deviation of the mean value. ....	20
Figure 6 Adsorption isotherm of Cr(VI) onto bare or stabilized Fe-Mn nanoparticles. Initial condition: Cr(VI) = 0 ~ 60 mg/L, nanoparticles = 0.27 g/L (Fe = 0.2 g/L, Mn = 0.07 g/L), , starch = 0.19 wt.%, CMC = 0.16 wt. %, pH = 6 ±0.1. Symbols : Experimental data; Lines : Langmuir model fitting. All data are duplicated, errors indicate the standard deviation of the mean value. ....	22
Figure 7 Cr(VI) removal efficiency for bare and starch stabilized Fe-Mn at pH range of 3 to 10. Initial condition: Cr(VI) = 5 mg/L, nanoparticle = 0.27 g/L ( Fe = 0.2g/L, Mn = 0.07 g/L), temperature = 23 °C) .....	24
Figure 8 Effect of competing ions on Cr(VI) adsorption on bare Fe-Mn nanoparticle. Initial condition: Cr(VI) = 5 mg/L = 0.1M, SO42- = 0.1 or 1 mM, PO43- = 0.1 mM or 1mM.....	26
Figure 9 Effect of competing ions on Cr(VI) adsorption on starch Fe-Mn nanoparticle. Initial condition: Cr(VI) = 5 mg/L = 0.1M, SO42- = 0.1 or 1 mM, PO43- = 0.1 mM or 1mM.....	26
Figure 10 Effect of humic acid on C(VI) adsorption. (a) bare Fe-Mn. (b) starch stabilized Fe-Mn. Initial Cr(VI) = 5 mg/L, nanoparticle = 0.27 g/L (Fe =0.2 g/L, Mn = 0.07 g/L).....	28
Figure 11 Breakthrough curve of starch stabilized Fe-Mn nanoparticles through a sandy loam soil bed. Nanoparticle = 0.27 g/L (Fe = 0.2 g/L, Mn = 0.07 g/L), starch = 0.19 wt. %, pH = 6.0. EBCT = 71 min, flow velocity = 0.15 mL/min .....	30

Figure 12 Cr(VI) concentration profiles in elution using DI water and starch stabilized Fe-Mn nanoparticle. Initial condition: Cr spiked soil = 87 mg/kg, nanoparticle = 0.27 g/L (Fe = 0.2 g/L, Mn = 0.07 g/L), starch = 0.19 wt. %, pH = 6.0-6.3. EBCT = 71 min, flow velocity = 0.15 mL/min..... 31

## List of Abbreviations

CMC	Carboxymethyl Cellulose
EPA	Environmental Protection Agency
EBCT	Empty bed contact time
Fe-Mn	Iron – Manganese oxide
FT-IR	Fourier Transform Infrared Spectroscopy
MCL	Maximum Contaminant Level
PV	Pore Volume
TCLP	Toxicity Characteristic Leaching Procedure
TOC	Total Organic Carbon
XPS	X-ray Photoelectron Spectroscopy

## Chapter 1. Introduction

Chromium is an essential nutrient for living species, it could be serious pollutant when accumulated at high levels due to the toxic and mutagenic properties of hexavalent chromium (Chad P. Johnston, 2014). In groundwater system, the dominant states of chromium is trivalent and hexavalent depends on reducing conditions. Hexavalent chromium exist as chromate in environment, it is much more harmful than trivalent species for its solubility and mobility, while trivalent chromate species are approximately insoluble in neutral pH (Mojdeh Oowlad, 2009). Trivalent and hexavalent chromium are convertible is aqueous phase, so U.S. Environmental Protection Agency set a Maximum Contaminant Level of 0.1 mg/L for total chromium in drinking water.

In nature water system, the dominant occurring form of chromium is trivalent species, trivalent chromium oxide is stable and very slow to react, other oxidation states contact with natural environment tend to be converted to the trivalent form (Barnhart, 1997). The expected background concentration of chromium is less than 10 µg/L (Peterson M, 1996). With the industry and technology development, the releasing in environment of chromium compounds has been continuously increasing (Yang Gao, 2011). To protect public health and the environment, the chromium discharge limit is regulated to be less than 50 µg/L for hexavalent chromium and 2 mg/L for total chromium by the U.S. Environmental Protection Agency (Baral A, 2002).

Various technologies such as electrocoagulation (Shaima S. Hamdan, 2014), ion exchange (Marinin, 2000), membrane filtration (Bessbousse, 2008), adsorption (M. Nameni, 2008) and electrochemical precipitation (Kurniawan, 2006) have been developed for chromium removal in water and groundwater, while the most promising method is adsorption for the significant advantages of low cost, easy operating, availability and high efficiency in comparison with other methods. (Mojdeh Oowlad, 2009). Iron based nanoscale sorbents are currently widely used material in chromate removal, it can be divided into two groups based on different chemistry: iron act as a sorbent or act as a reducing agent follow by precipitation of trivalent chromium.

This research focus on the investigation of hexavalent chromium immobilization in simulated groundwater by a bare/stabilized Iron-Manganese binary oxide nanoparticle. Which includes, (1) synthesis of Iron-Manganese nanoparticle and their efficiency in Cr (VI) removal, (2) the mechanism of Cr(VI) adsorption onto Iron-Manganese nanoparticles, (3) Cr(VI) immobilization efficiency by stabilized Fe-Mn nanoparticle in soil test. To meet the research object, a series of batch and column test were conducted.

## **Chapter 2 Chromate immobilization in Soil and Groundwater using stabilized Fe-Mn nanoparticles**

To demonstrate the adsorption behavior of Cr(VI) onto Fe-Mn nanoparticles, a series of batch and column test were conducted. Batch test with a Cr(VI) concentration range (1mg/L – 100mg/L) were carried out with a fixed nanoparticle concentration (0.2g/L as Fe), while the effect of varies environmental conditions (pH, ligands and reaction time) on removal efficiency were investigated. The adsorption mechanism of chromium adsorption on Fe-Mn nanoparticle were characterized with the combination of FTIR and XPS measurement. The immobilization of Hexavalent chromium in soil using starch stabilized Fe-Mn nanoparticles was evaluated batch and fixed bed column tests.

### 2.1. Introduction

Chromium is a transition metal with atomic number of 24, which is an essential nutrient for living species, but if accumulated at high concentration, it could be a serious pollutant. Like other transition metal, chromium exist at varies oxidation states (), in nature water only trivalent and hexavalent is table. Trivalent chromium occurs as  $\text{Cr}^{3+}$ ,  $\text{Cr}(\text{OH})^{2+}$  and  $\text{Cr}(\text{OH})_4^-$  in aqueous phase/,  $\text{Cr}(\text{OH})_3$  precipitation predominates in solution at a neutral pH range (6 - 12). In contrast, hexavalent chromium exist as much more soluble anions like  $\text{HCrO}_4^-$ ,  $\text{CrO}_4^{2-}$ , or  $\text{Cr}_2\text{O}_7^{2-}$  at different pH and concentration

## 2.2. Material and methods

### 2.2.1. Chemical and materials

All chemicals used in this research were of analytical grade or higher. Including  $\text{KMnO}_4$  (Acros Organics, Morris, NJ, USA),  $\text{FeCl}_2 \cdot 4\text{H}_2\text{O}$  (Acros Organics, Morris Plains, NJ, USA),  $\text{Na}_2\text{CrO}_4 \cdot 4\text{H}_2\text{O}$  (J. T. Baker, PA, USA), soluble potato starch (Sigma-Aldrich, Milwaukee, WI, USA). Carboxymethyl Cellulose (CMC, Sigma-Aldrich, Milwaukee, WI, USA), NaOH (Fisher Scientific, Pittsburgh, PA, USA) and Hydrochloric acid (Mallinckrodt Chemicals, St, Louis, MO, USA).

### 2.2.2. Synthesis of nanoparticles

Bare and Stabilized (with starch or CMC) Fe-Mn binary oxide nanoparticles were synthesis following the previous research in our lab (Byungryul An, 2012). At any volume of glass flask, nanoparticle was synthesized with a fix concentration of 0.2 g/L Fe and 0.07 g/L Mn. The stock solution of starch (1 wt. %) and CMC (1 wt. %) were prepared prior to experiment. Then, take a various volumes of starch or CMC stock solution to yield a desire concentration of stabilizer with deionized water ( $18.2 \Omega \text{ cm}^{-1}$ ), DI water was purified with  $\text{N}_2$  gas for 30 minutes prior to use. Then 10 ml of 6.336 g/L  $\text{FeCl}_2$  was added to solution and mixed for 10 min under vigorous magnetic stirring. The reaction was initialed with adding 10 mL of 2.65 g/L  $\text{KMnO}_4$  solution, then increase the solution pH to  $\sim 7.5$  immediately with 2 M NaOH. The Fe-Mn nanoparticles were obtained after 1 hour shaking on a platform shaker at 200 rpm.

### 2.2.3. Preparation of Cr(VI) spiked soil

Sandy loam soil used in this experiment was obtained from a local farm near Auburn University. The raw soil was washed with tap water to remove all soluble components and then

air – dried at room temperature. Before use, the sandy loam soil was sieved with a 2 mm sieve. The soil elementary analysis was conducted in the Soil Testing Laboratory at Auburn University following U.S.EPA 3050B Method. The soil characteristics was given in Table 2-1.

Table 1 Characteristic of Loamy sandy soil used in experiment

Textural Class	pH	H <sub>2</sub> O	CEC meq/100 g	OM %	Ca ppm	K ppm	Mg ppm	P ppm	Al ppm	As ppm	B ppm
Loamy Sand	6.77	0	0.5	0.1%	59	6	14	<0.1	12	<0.1	2

Ba ppm	Cd ppm	Cr ppm	Cu ppm	Fe ppm	Mn ppm	Mo ppm	Na ppm	Ni ppm	Pb ppm	Zn ppm
2	<0.1	<0.1	4	4	2	<0.1	18	<0.1	<0.1	4

To prepare Cr(VI)-loaded soil. 200 g of air-dried sandy loam soil was added in 1 L of Chromate stock solution (200 mg/L as Cr(VI)). The mixture was shaken for 1 week to reach equilibrium, pH was maintained at  $6 \pm 0.1$  with 1 M NaOH and 1 M HCl. The Cr(VI) uptake was 87 mg of Cr(VI)/kg of dry soil.

### 2.2.3. Characterization of Fe-Mn nanoparticles

The surface functional groups of particles before and after Cr(VI) adsorption were characterized by Fourier Transform Infrared Spectroscopy (FTIR, Bruker, Germany) with a scanning range of 4000–400 cm<sup>-1</sup> and 4 cm<sup>-1</sup> resolution through KBr pellet method. The elemental composition and oxidation state of samples were analysed on an X-ray photoelectron

spectroscopy (XPS, AXIS-Ultra, Kratos Analytical), which was conducted using monochromatic Al K $\alpha$  radiation (225 W, 15 mA, 15 kV) and low-energy electron flooding for charge compensation. All the peaks were calibrated using C 1s hydrocarbon peaked at 284.80 eV in order to compensate for surface charges effects. All results were analysed with Casa-XPS software package. Two types of measurements were performed: (1) low-resolution measurement was conducted to obtain the survey spectra which present all element on the particle surface, and (2) high-resolution measurement to identify the oxidation states of target elements.

The zeta potential ( $\zeta$ ) data was collect on Zetasizer nano ZS (Malvern instruments, UK) under pH range of 3 to 10. The experiments were conduct using a 0.75 mL folded-capillary cell at 25 °C. Bare Fe-Mn nanoparticles were sonicated prior to measurement using a sonicator (550 Dismembrator, Fisher Scientific, Pittsburg, PA, USA).

#### 2.2.4 Cr(VI) removal in aqueous phase: Batch test

A series of kinetic test in batch were carried out to investigate the adsorption rate of chromate onto Fe-Mn nanoparticles. Bare, starch (0.19 wt. %) and CMC (0.16wt. %) stabilized nanoparticles were synthesis separately at 0.27 g/L as Fe-Mn with adding of 500 mg/L of Cr(VI) stock solution. Yield an initial Cr(VI) concentration of 5 mg/L, pH of mixture was maintained at  $6 \pm 0.1$  with intermittent adjustment using 0.1 M NaOH and 0.1 M HCl. . Reactions were performed on a platform shaker at 200 rpm. 4 mL of mixtures was sampled at predetermined time. Collected samples were vacuum filtrated with a 25 nm mixed cellulose esters membrane (MF- Millipore Corporation, Billerica, MA, USA) to remove all particles. Filtered samples were diluted to 5 folds in tube with 0.1 M HNO $_3$  prior to analysis with ICP-AES.

To investigate the stabilizer dosage on chromate removal efficiency, a series of batch equilibrium tests were conducted. At a fixed Fe and Mn concentration (0.27 g/L, Fe = 0.2 g/L and Mn = 0.07 g/L), initial Cr(VI) concentration of 5 mg/L, a series of starch concentrations (0, 0.05, 0.1, 0.15, 0.19, and 0.21 wt.%) were yielded with various volumes of starch stock solution and DI water. The pH was adjusted to  $6 \pm 0.1$  during the whole reaction process. To reach a fully equilibrium state, the mixtures were allowed to react for 2 hours on a platform shaker at 200 rpm.

Batch Isotherm tests of bare and stabilized (starch and CMC) Fe-Mn were conducted to compare the effect of different stabilizers on chromate removal efficiency. Batch experiments were performed in 250 mL conical flasks with a particle suspension volume of 140 mL, starch = 0.19 wt. %, CMC = 0.16 wt. %, particle concentration = 0.27 g/L (Fe = 0.2 g/L, Mn = 0.07 g/L), Initial Cr (VI) = 0 ~60 mg/L. pH was maintained at  $6 \pm 0.1$  during the whole process by intermittent adjustment with 0.1 M NaOH and 0.1 M HCl.

The effect of pH was determined at a pH range of 3 to 10. The effect of competing ions like sulfate and phosphate on chromate removal was introduced at pH 6. The effect by humic acid (0 to 20 mg/L as TOC) was also determined in batch kinetic tests.

### 2.2.5 TCLP leaching Test

To compare the Cr(VI) leaching from soil before and after treated with stabilized nanoparticle. The toxicity characteristic leaching procedure (TCLP) was applied following EPA method 1311. The soil was treated with starch Fe-Mn then freeze-dried. The dried sample was mixed with the TCLP fluid #1 (0.57% glacial acetic acid + 0.64 N NaOH, result in a mixture

with pH  $4.93 \pm 0.05$ ) at a solid to solution ratio of 1: 10 ( 1g soil and 10 mL of TCLP fluid #1). The mixture was allowed to react for 18 hours on a platform rotator at 30 rpm.

#### 2.2.6 Immobilization of Cr(VI) in soil

To investigate the efficiency of stabilized Fe-Mn nanoparticle for immobilization of Cr(VI) in contaminant soil. A series of batch kinetic test were conducted mixing the Cr(VI) spiked soil and starch stabilized Fe-Mn nanoparticles. Test was initialed by mixing 1 g of contaminant soil with 10 mL of nanoparticle suspension in a 20 ml glass bottle, the pH was adjust to  $6.0 \pm 0.1$  with 0.1 M NaOH and 0.1 M HCl. The mixture was rotated for 48 hous to reach equilibrium on a platform shaker at 30 rpm. After reaction, the mixtures were centrifuged at 6500 rpm (5857g of RCF) for 10 minutes, supernatants were filtered through a 25 nm membrane to removal all particles, then the filtrate was diluted to acceptable level with 0.1 M HCl for analysis using ICP-OES.

#### 2.2.7 Column tests

To evaluate the breakthrough and mobility of stabilized Fe-Mn nanoparticles in soil, fixed bed column tests were conducted. The column was set up with a Plexiglas clolumn (inner diameter = 1.0 cm, length = 10 cm; Omnifit, Cambridge, UK), 10 g of sandy loam soil was packed in the column, result in a soil porosity of 0.34, pore volume of 2.2 mL and a bulk bed volume of 6.4 mL. The starch stabilized Fe-Mn nanoparticle was pass through the column at a flow rate of 0.09 mL/min in down flow mode, which result in a pore velocity of  $5.6 \times 10^{-3}$  cm/s and empty bed contact time (EBCT) of 71.1. The nanoparticle suspension was pumped with a Harvard Apparatus PHD 2000 syringe pump (Plymouth Meeting, PA, USA), the effluent was

collect with a fraction collector (Eldex laboratories, Napa, CA). To insure the hydrodynamic conditions of column, a tracer test was performed with KBr solution (50 mg/L as Br<sup>-</sup>) under identical conditions.

In the same column, Cr(VI) immobilization tests were conducted to evaluate the nanoparticle efficiency. 10 g Cr(VI) spiked soil was packed in the column. Then the column pumped with 20 pore volume of starch stabilized Fe-Mn nanoparticle at a flow rate of 0.09 mL/min. Cr(VI) in effluent was determined in two different methods. To determine total chromium, 5 M of HNO<sub>3</sub> was added to dissolve all particles then analyzed for Chromium. To determine the soluble chromium, the samples was filtered through a 25 nm membrane to removal all particles, the filtrate was acidified with 0.1 M HNO<sub>3</sub> then analyzed for chromium. For comparison, parallel test was conducted with alter the nanoparticle suspension with DI water under otherwise identical conditions.

#### 2.2.8. Analytical methods

Total chromium concentration were determined with ICP-AES (Varian 710-ES). Before analysis, samples were filtered with 25nm membrane and then diluted with 0.1 M HCl. Cr(VI) concentration was determined with Ultraviolet – Visible spectroscopy (UV-Vis). Humic acid analysis was conducted a TOC Analyzers. Zeta potential was measured using a Zetasizer (Malvern, Zen3600, UK).

## Chapter 3 Result and discussion

### 3.1. Characterization of adsorbent

**Fig. 1** shows the FT-IR spectra of bare and starch stabilized Fe-Mn nanoparticles before and after adsorption of Cr(VI). The peak at 3300–3400  $\text{cm}^{-1}$  and  $\sim 1630 \text{ cm}^{-1}$  is assigned to vibration of hydroxyl groups (O–H) and bonded water (H–O–H) (Xiong L, 2011). For starch-stabilized Fe-Mn, the band at 2924  $\text{cm}^{-1}$  belongs to C–H ( $\text{CH}_2$  deformation), while the peak at 1372 and 1499  $\text{cm}^{-1}$  is consistent with C–O–H bending and  $-\text{CH}_2$  twisting vibration, respectively (Kizil, I rudayaraj, & Seetharaman, 2002), indicating successfully coating of starch onto Fe-Mn. In addition, After adsorption, the new peaks locate at 935 and 620  $\text{cm}^{-1}$  is contributed to the stretching vibration of Cr=O and Cr–O, which come from  $\text{HCrO}_4^-$ ,  $\text{CrO}_4^{2-}$  or  $\text{Cr}_2\text{O}_7^{2-}$  and indicates that Cr(VI) adsorbed onto the nanoparticles (Haisa, 1993). Moreover, there is a shift for –OH from 3399 to 3419  $\text{cm}^{-1}$  for bare Fe-Mn, and from 3424 to 3394  $\text{cm}^{-1}$  for starch stabilized Fe-Mn, suggesting Cr(VI) interacted with hydroxyl groups in the adsorption process.

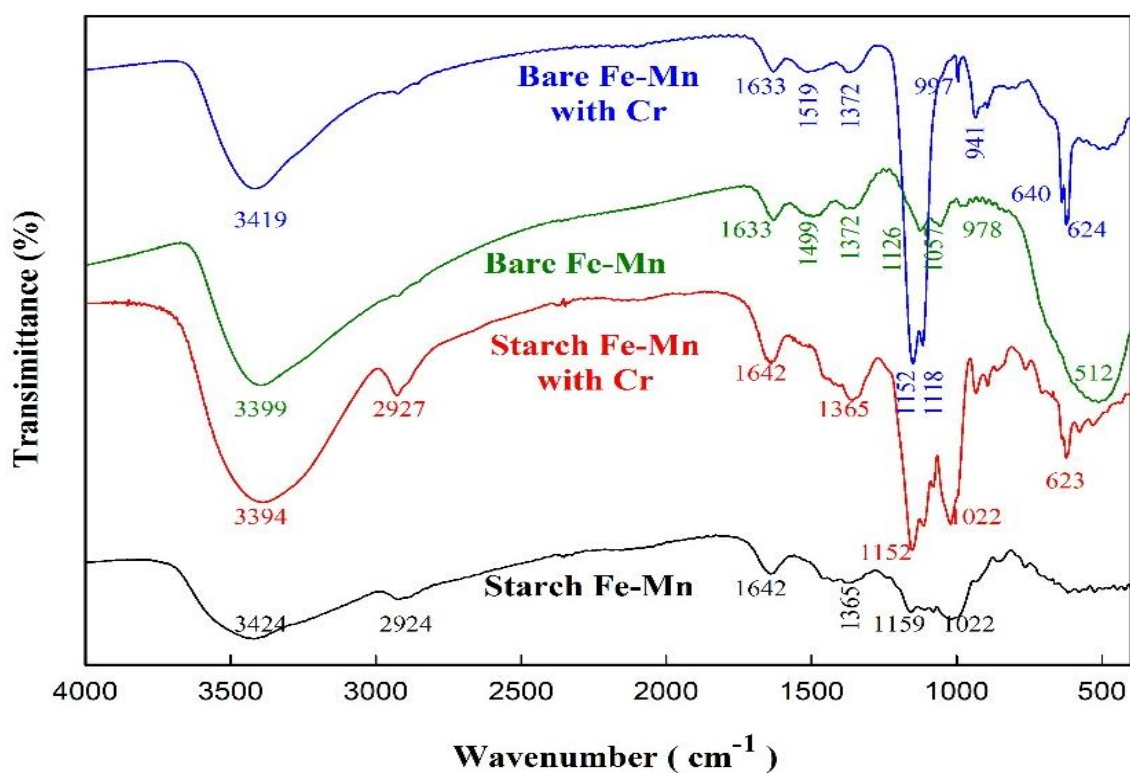
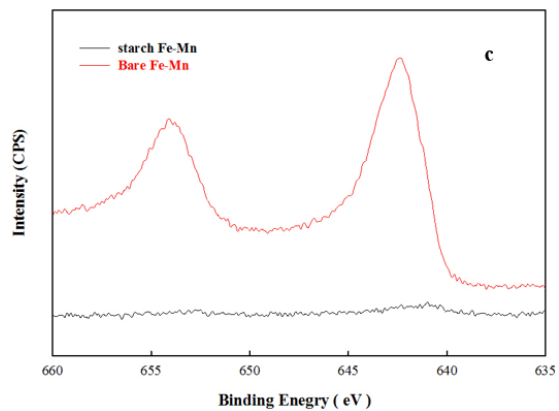
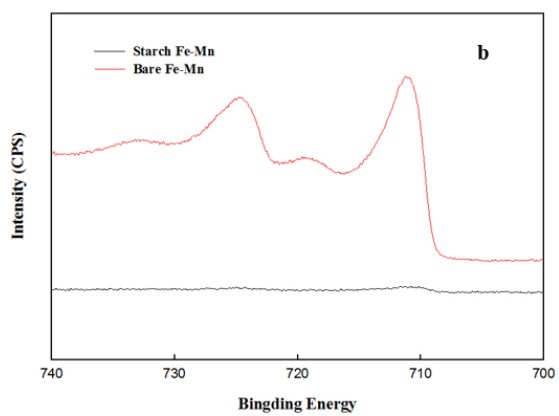
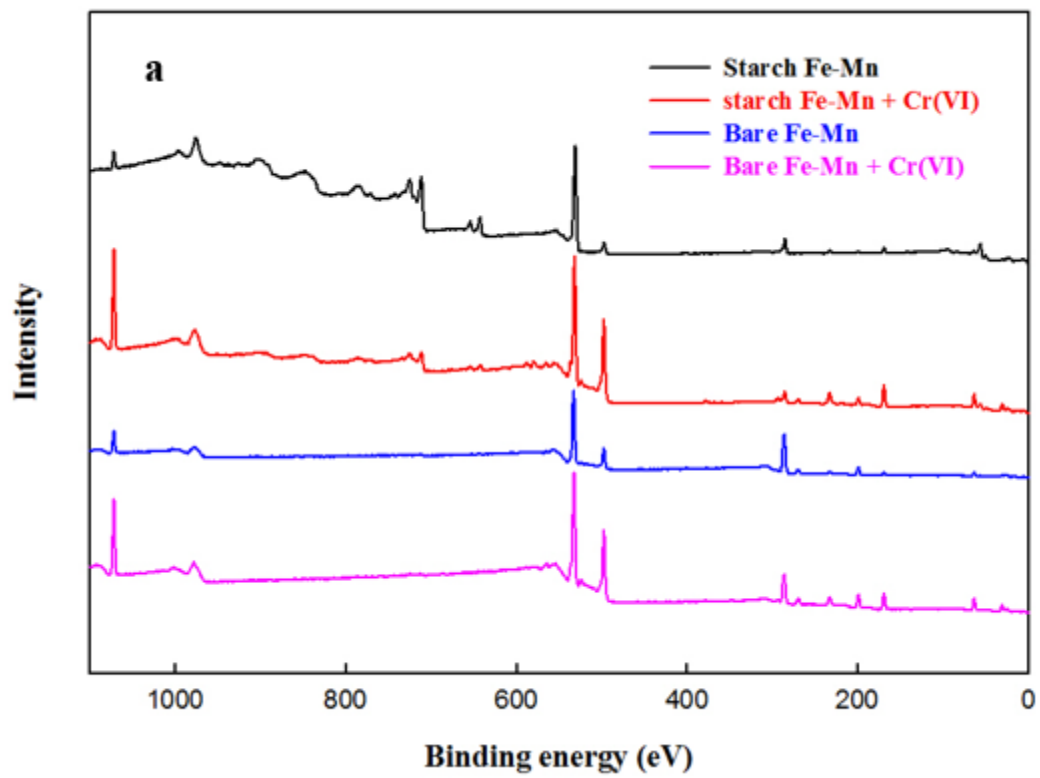


Figure 1 FT-IR spectra of bare and starch stabilized Fe-Mn nanoparticles before and after Cr(VI) adsorption.

Fig.2 presents the XPS spectra of bare and stabilized Fe–Mn before and after adsorption. The main elements of bare Fe–Mn nanoparticles are Fe, Mn and O. While after starch coated, C percentage (58.7%) greatly enhanced as starch was an organic matter with large molecular weight. After Cr(VI) adsorption, Cr 2p peaks appeared both for bare and starch stabilized Fe–Mn, indicating Cr(VI) attached onto the nanoparticles. In the high resolution of Fe 2p spectra (Fig .2b), the peaks at about 724 and 711 eV belong to the Fe 2p<sub>1/2</sub> and 2p<sub>3/2</sub> core-level XPS peaks for Fe<sub>2</sub>O<sub>3</sub> (Fig. 2c) (Kontos A I, 2009). The peaks at about 654 and 642 eV are assigned to the Mn 2p<sub>1/2</sub> and 2p<sub>3/2</sub> spin-orbit peaks of MnO<sub>2</sub>, which is consistent with MnO<sub>2</sub> (Fig. 2c) (Lei Z, 2012). In addition, all the attached Cr on the materials is detected as Cr(VI) (at ca. 580 eV) and no Cr(III) can be found in the high resolution of Cr 2p spectra after adsorption (Fang J, 2007), indicating Cr(VI) was just adsorbed onto Fe-Mn nanoparticles and no reduction occurred, which is in accordance with the experimental results. No obvious peaks of Fe 2p, Mn 2p and Cr 2p for starch stabilized Fe-Mn observed in the high resolution spectra was due to large amount of starch coating on the surface of the nanoparticles.



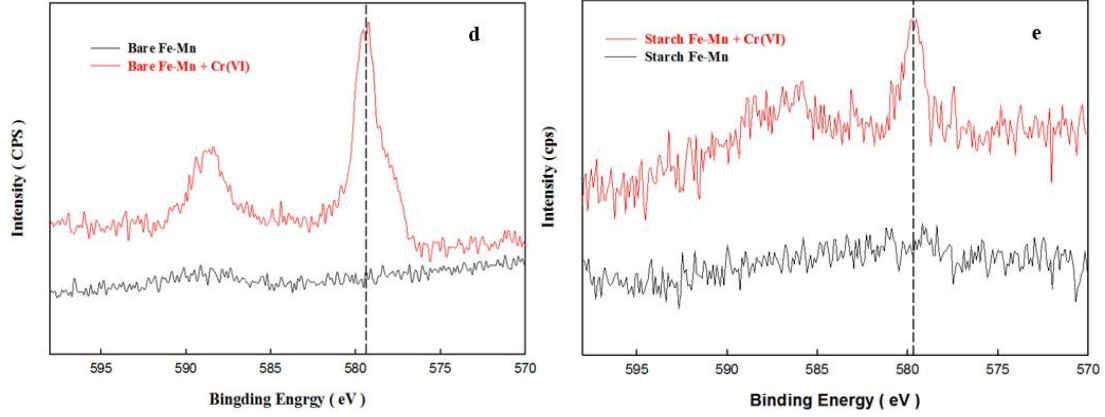


Figure 2 XPS analysis of bare and stabilized Fe-Mn before and after adsorption of Cr(VI).  
**(a)** Survey spectra; high resolution of **(b)** Fe 2p, **(c)** Mn 2p and **(d)** Cr 2p.

Based on FT-IR and XPS analyses, the adsorption mechanism of Cr(VI) on Fe-Mn processes as Eqns 1–4, and electrostatic attraction plays the primary role.

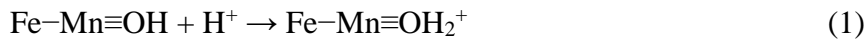


Fig. 3 represent the zeta potential of bare, starch or CMC stabilized Fe-Mn nanoparticle. For bare particle, the zeta potential are +35 mV at pH 3 and -30 mV at pH 10, the point of zero charge is about 5.9, same value was reported for Fe-Mn prepared in similar method (Gaosheng Zhang, 2007). From previous report, ZPC of amorphous  $\text{Fe}(\text{OH})_3$  (C. Su, 2000), synthetic birnessite  $\delta\text{-MnO}_2$  (Sphsite, 1989) (W.F. Tan, 2008), synthetic magnetite  $\text{Fe}_3\text{O}_4$  (Liang, 2012),  $\beta\text{-MnO}_2$  (Zhao, 2010) were 8.5, 15 to 2.5, 6.1, and 4.2, respectively.

Coating with 0.19 wt. % of starch, zeta potential of Fe-Mn was shielded largely, zeta potential change in whole pH range (3-10) is only +2 to -6. It was reported that the dense H-bond of neutral polymer will result in a buffer effect which diminished the surface charge (Biggs, 2006).

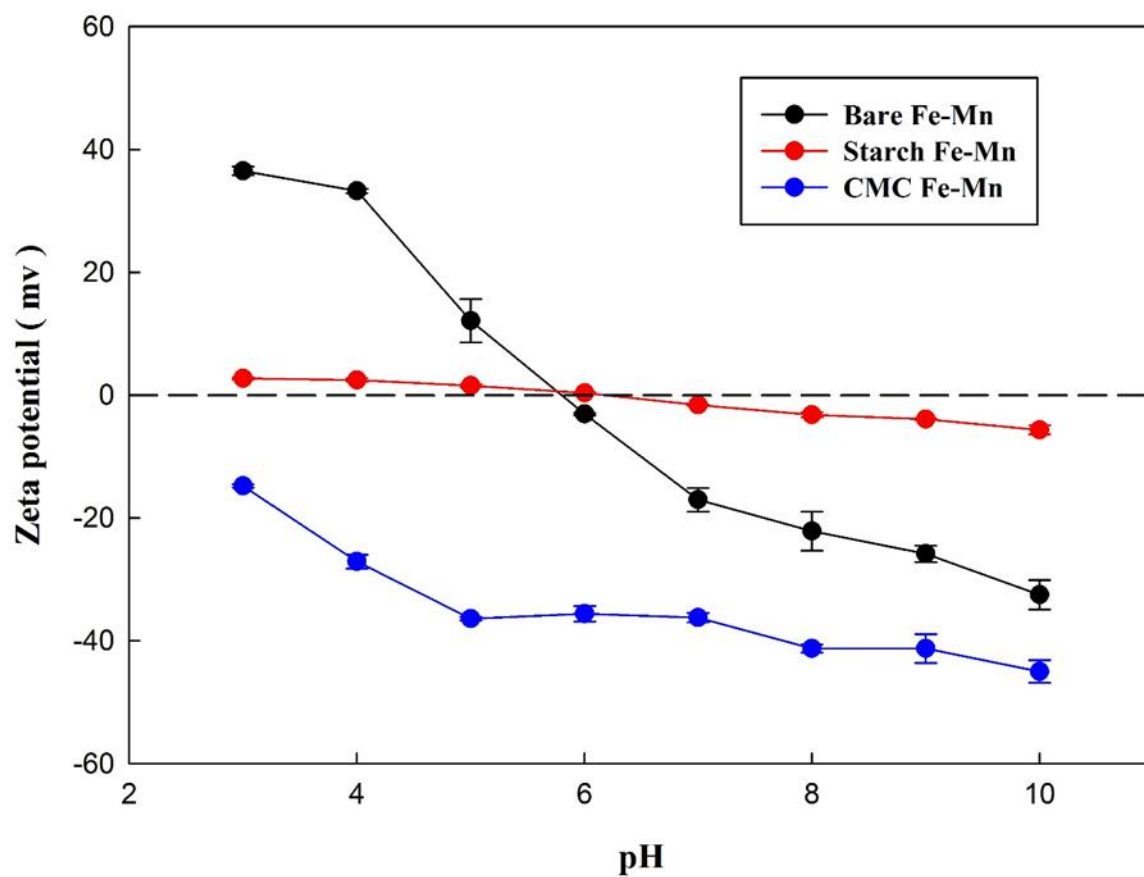


Figure 3 Zeta potential of bare, starch or CMC stabilized Fe-Mn as a function of pH. Initial condition: Cr(VI) = 5 mg/L, starch = 0.19 wt. %, CMC = 0.16 wt. %, Fe = 0.2 g/L, Mn = 0.07 g/L.

### 3.2 Stabilizer dosage effect on Cr(VI) removal

Fig. 4 shown the remaining percentage of Cr(VI) as a function of starch concentration. Bare Fe-Mn nanoparticle shows a much higher removal efficiency (95%). With starch (0.05, 0.1, 0.15, 0.19, and 0.21 wt. %), the removal efficiency reach the maximum value of 92% at 0.19 wt. % of starch. Referred to stability analysis, Fe-Mn nanoparticle was fully stabilized by starch at concentration of 0.19 wt. %. Stabilization of Fe-Mn resulted in fully dispersible and smaller nanoparticles, while the partially stabilized Fe-Mn will trend to form coagulation and precipitation (Byungryul An, 2012). For partially stabilized Fe-Mn nanoparticles, the surface function group may be blocked by starch, then result in a lower removal efficiency than bare particle. Referred the result of zeta potential, Fe-Mn nanoparticle surface charge Fe-Mn was narrowed to a small range. The presence of starch did not show any advantage on adsorption capacity and reaction rate.

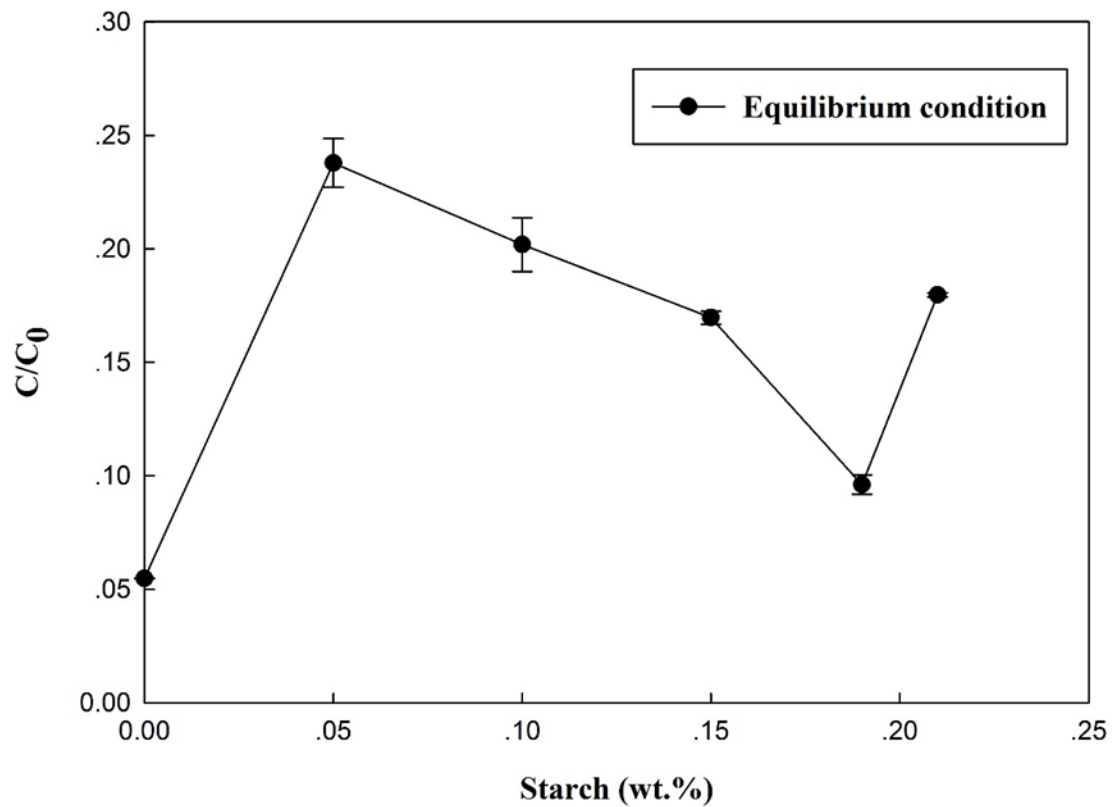


Figure 4 Chromate removal efficiency as a function of various starch concentration. Initial condition: Cr(VI) = 10 mg/L, pH = 6 ± 0.1, Fe = 0.2 g/L, Mn = 0.07 g/L. (All samples were made in duplicated)

### 3.3 Kinetic of Cr(VI) removal by Fe-Mn nanoparticle

Figure 5 shows the comparison kinetics of chromate adsorption onto bare, starch and CMC stabilized Fe-Mn nanoparticles. For bare and CMC stabilized nanoparticles, equilibrium condition was reached in less than 30 minutes, two hours for starch stabilized nanoparticle. At this condition, the removal efficiency was 99%, 98%, 18% for bare, starch and CMC stabilized Fe-Mn nanoparticles, respectively.

Pseudo second-order model was applied to fit the kinetic data:

$$\frac{dq_t}{dt} = k(q_c - q_t)^2 \quad (5)$$

Where  $K$  is the rate constant of sorption (g/mg-min),  $q_c$  is the amount of sorption at equilibrium condition,  $q_t$  is the amount of sorption at time  $t$ ,  $t$  is the reaction time. The calculated parameter data was given in table 2.

Table 2 Calculation of pseudo second order model

	k (g/mg min)	Rsqr
Bare Fe-Mn	0.5732	0.9992
Starch Fe-Mn	0.0736	0.9928
CMC Fe-Mn	0.3597	0.9767

All plots are well fitted with pseudo second order equation. The adsorption rate following the order of bare Fe-Mn > CMC Fe-Mn > starch Fe-Mn. CMC Fe-Mn exhibited a low removal efficiency but a fast reaction rate. Compare with neutral charged starch, CMC stabilizer will make Fe-Mn nanoparticle negatively charged, the electrostatic repulsion force between particles introduced by negative charge will promote the smaller particle size and more stable distribution

(Byungrlyul An, 2012). Considered the negative charge of chromate anion, there will be no surprise for the low removal efficiency and high adsorption rate. For starch coated Fe-Mn nanoparticle, presence of stabilizer did not show any advantage of removal efficiency, same with the isotherm result given in Figure 4.

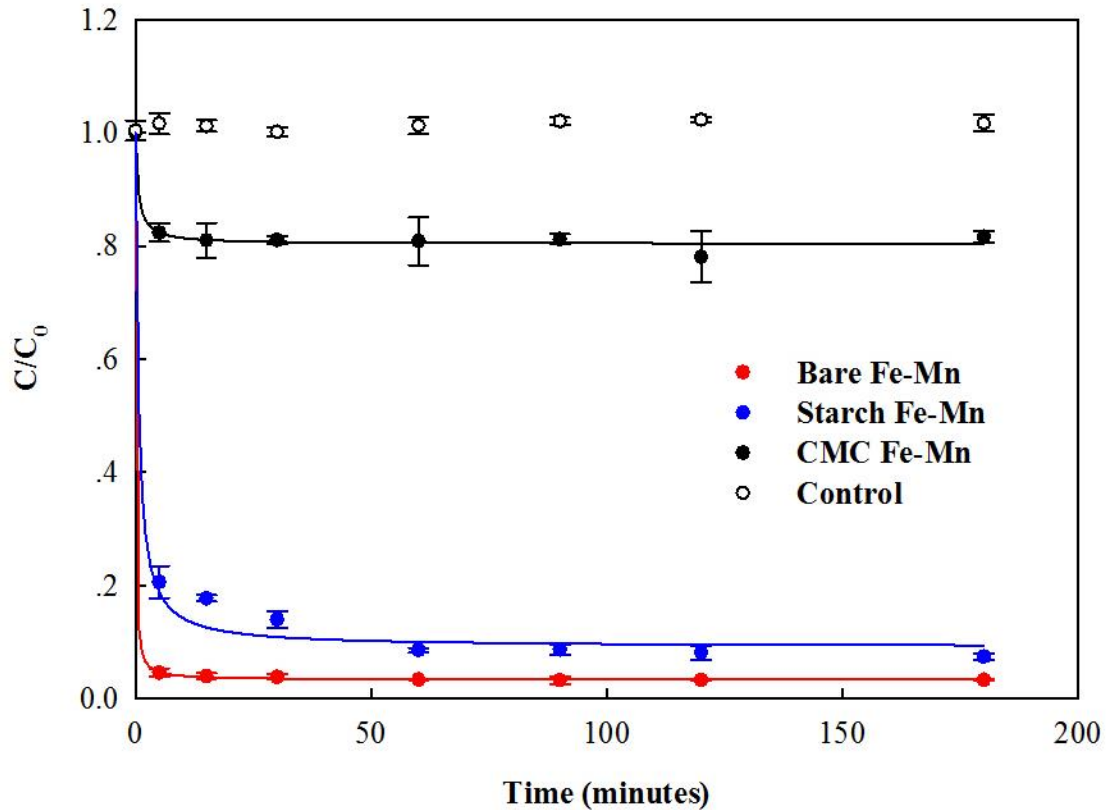


Figure 5 Kinetic of Cr(VI) removal with bare or stabilized Fe-Mn nanoparticles.  $C_0$  and  $C$  represent the initial concentration and concentration at time  $t$  of Cr(VI), respectively. Initial Cr(VI) = 5 mg/L, nanoparticles = 0.27 g/L (Fe = 0.2 g/L; Mn = 0.07 g/L), starch = 0.19 wt.%, CMC = 0.16 wt. %, pH =  $6 \pm 0.1$ . Symbols : Experimental data; Lines : Pseudo second order model. All data are duplicated, errors indicate the standard deviation of the mean value.

### 3.4. Adsorption isotherm of Cr(VI)

At pH 6, Isotherm data of Cr(VI) adsorption onto bare, starch or CMC stabilized Fe-Mn nanoparticles were obtained. Figure 6 shows the Langmuir model fitting of each particle.

$$q = \frac{bQc_e}{1+bc_e} \quad (6)$$

Where  $q_e$  is the equilibrium concentration of Cr(VI) in solid phase.  $C_e$  is the equilibrium concentration in aqueous phase,  $b$  is the Langmuir affinity coefficient (L/mg),  $Q$  is the maximum adsorption capacity (mg/g).

Table 3 Langmuir model parameter for bare, starch and CMC Fe-Mn

Langmuir Model	Q (mg/g)	b (L/mg)	Rsqr
Bare	59	0.69	0.9704
Starch	54	0.92	0.9722
CMC	2	0.23	0.9900

Fit the data with Sigma plot software, the Langmuir parameters were given in Table 3.

Maximum adsorption capacities are 59, 54, and 2 mg/g for bare, starch and CMC stabilized Fe-Mn nanoparticle. Although directly comparison of Q value is meaningless, consider the different reaction condition, we can say both bare Fe-Mn and Starch Fe-Mn exhibited much higher adsorption capacity than maghemite, 19.2 mg/g at pH of 2-3, diatomite, 11.55mg/g (Dantas, 2001), anatase, 14.56mg/g (Weng, 1997),  $\alpha$ -Fe<sub>2</sub>O<sub>3</sub>, 30 mg/g (Changyan Gao, 2012).

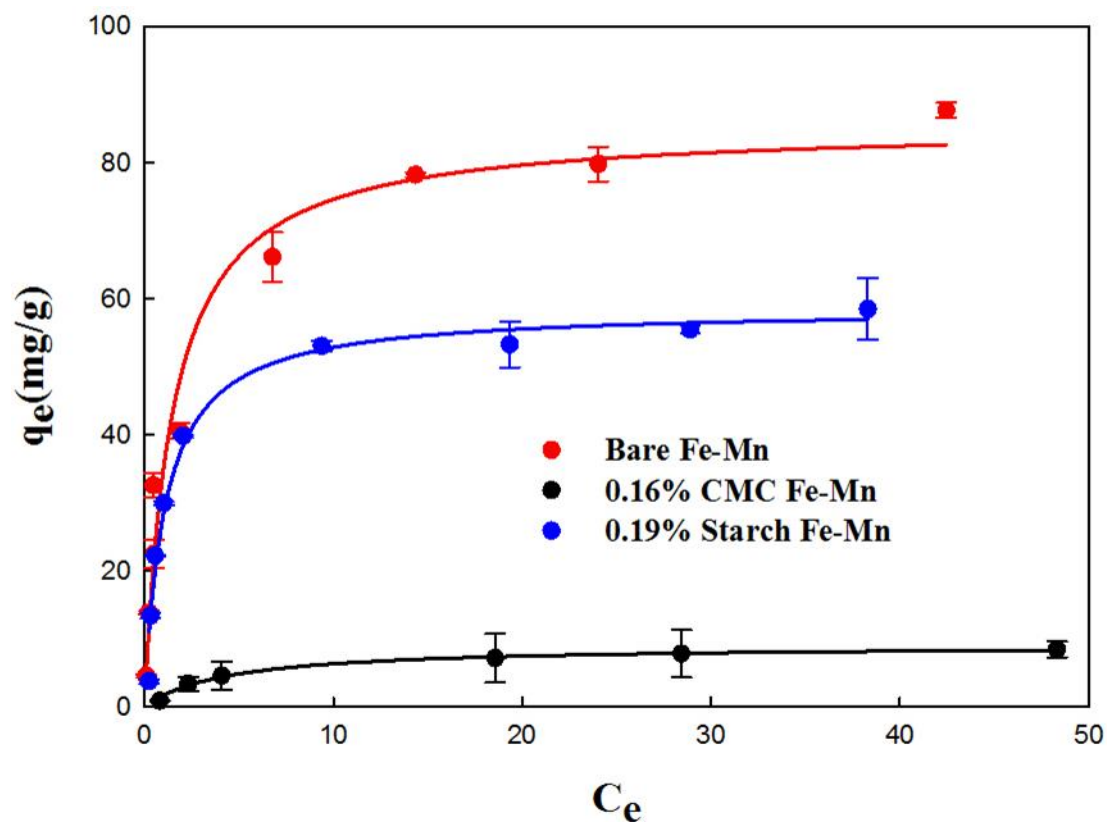


Figure 6 Adsorption isotherm of Cr(VI) onto bare or stabilized Fe-Mn nanoparticles. Initial condition: Cr(VI) = 0 ~ 60 mg/L, nanoparticles = 0.27 g/L (Fe = 0.2 g/L, Mn = 0.07 g/L), starch = 0.19 wt.%, CMC = 0.16 wt. %, pH = 6 ± 0.1. Symbols : Experimental data; Lines : Langmuir model fitting. All data are duplicated, errors indicate the standard deviation of the mean value.

### 3.4. Effect of pH and competing ions

Solution pH can highly affects the chromate species and nanoparticle surface charge. The pH effect on adsorption of Cr(VI) on to bare and starch stabilized Fe-Mn nanoparticles was investigated at pH range of 3 to 10. Fig. 7 present the chromate removal efficiency for bare and starch stabilized Fe-Mn nanoparticles. It was found that both bare and starch stabilized Fe-Mn exhibited higher removal efficiencies (98% and 97%) from pH 3 to 6, respectively. the efficiency dropped sharply from pH 7, and less than 20% chromate was removed at pH 10 for both bare and starch stabilized Fe-Mn nanoparticles.

Based on previously report, the dominant species of Cr(VI) is  $\text{HCrO}_4^-$  (> 75%) at  $\text{pH} < 6$  and  $\text{CrO}_4^{2-}$  (> 75%) (R. K. Tandon, 1983), on the other hand, the point of zero charge (ZPC) was about 6 for both bare and starch stabilized Fe-Mn nanoparticles, thus the positive charged Fe-Mn nanoparticles will be favorable to adsorb Cr(VI) at  $\text{pH} < 6$ . From pH 7 to 10, the negatively charged Fe-Mn nanoparticles will trend to restrict the adsorption of Cr(VI) onto nanoparticle surface.

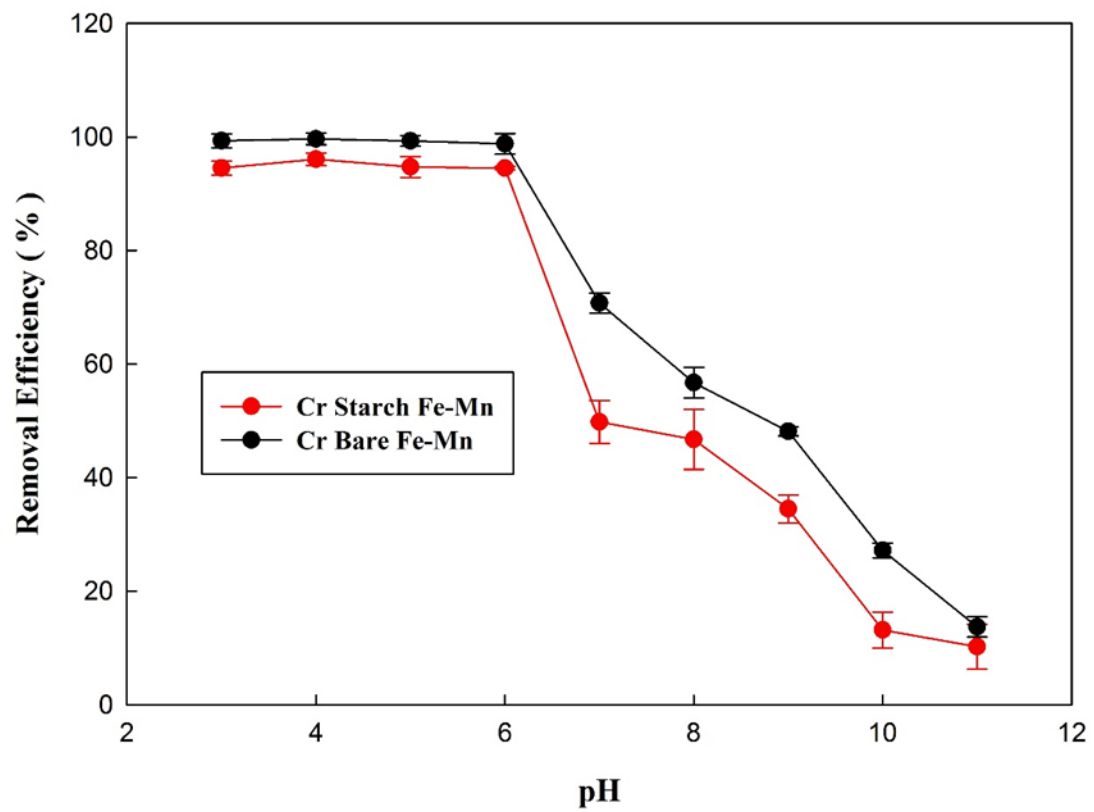


Figure 7 Cr(VI) removal efficiency for bare and starch stabilized Fe-Mn at pH range of 3 to 10.

Initial condition: Cr(VI) = 5 mg/L, nanoparticle = 0.27 g/L ( Fe = 0.2g/L, Mn = 0.07 g/L),

temperature = 23 °C)

### 3.5 Effect of competing ions

To test the specific selectivity of starch stabilized Fe-Mn nanoparticles, common competing ions  $\text{SO}_4^{2-}$  and  $\text{PO}_4^{3-}$  were introduced at concentration of 0.1 mM and 1 mM, respectively. Fig. 8 shows the test for bare particle, in the presence of 0.1 mM and 1mM  $\text{SO}_4^{2-}$ , the removal efficiency slightly dropped to 95% and 85% from 98%, while the value for  $\text{PO}_4^{3-}$  were 12% and 5%, respectively. Fig. 9 shows the result for starch stabilized particle. The presence of 0.1 mM and 1 mM  $\text{SO}_4^{2-}$  reduced the removal efficiency to 85% and 80%, while the value for  $\text{PO}_4^{3-}$  were 73% and 34%. Based on previous result, the main mechanism of Cr(VI) adsorption on Fe-Mn surface is electrostatic attraction force, the competing ions  $\text{SO}_4^{2-}$  and  $\text{PO}_4^{3-}$  with higher negative charge will strongly compete the surface adsorption site on Fe-Mn surface. After coating with stabilizer, the buffer effect of starch shielded the core Fe-Mn (Byungryul An, 2012) from charge sensitive. This finding indicates that starch coating offer greater selectivity of Fe-Mn nanoparticles toward Cr(VI).

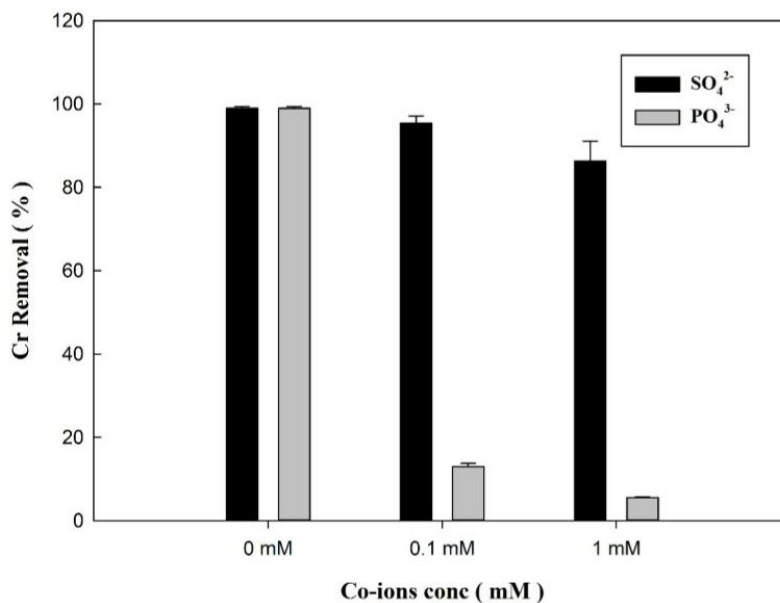


Figure 8 Effect of competing ions on Cr(VI) adsorption on bare Fe-Mn nanoparticle. Initial condition: Cr(VI) = 5 mg/L = 0.1M, SO<sub>4</sub><sup>2-</sup> = 0.1 or 1 mM, PO<sub>4</sub><sup>3-</sup> = 0.1 mM or 1mM.

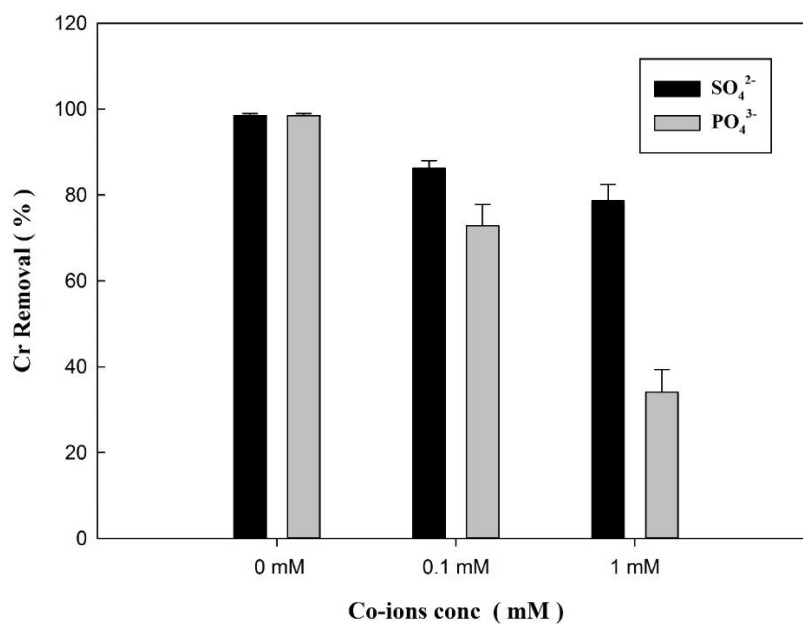


Figure 9 Effect of competing ions on Cr(VI) adsorption on starch Fe-Mn nanoparticle. Initial condition: Cr(VI) = 5 mg/L = 0.1M, SO<sub>4</sub><sup>2-</sup> = 0.1 or 1 mM, PO<sub>4</sub><sup>3-</sup> = 0.1 mM or 1mM.

### 3.6 Effect of humic acid

Humic acid (HA) is ubiquitously in environment, their variety of functional group may influence adsorption of heavy metal on nanomaterials (Wangwang Tang, 2014). Previous study indicated that HA plays an important roles on chromium adsorption on iron oxides nanoparticles (Jiang W. J., 2013). The effect of humic acid was investigated kinetic batch tests. The adsorption of Cr(VI) on Fe-Mn at varies HA concentration is presented in Fig. 10. It was reported that the presence of HA may compete the adsorption site on iron oxide surface with Cr(VI), but for bare Fe-Mn nanoparticles, the effect is negligible, from 0 to 10 ppm (as TOC) of HA, the Cr(VI) removal efficiency remains table.

Similar with bare particles, starch stabilized Fe-Mn can also exhibit comparable removal efficiency in the presence of 5 ppm HA, the removal efficiency dropped to 76% from 96 when HA concentration was increased to 20 mg/L.

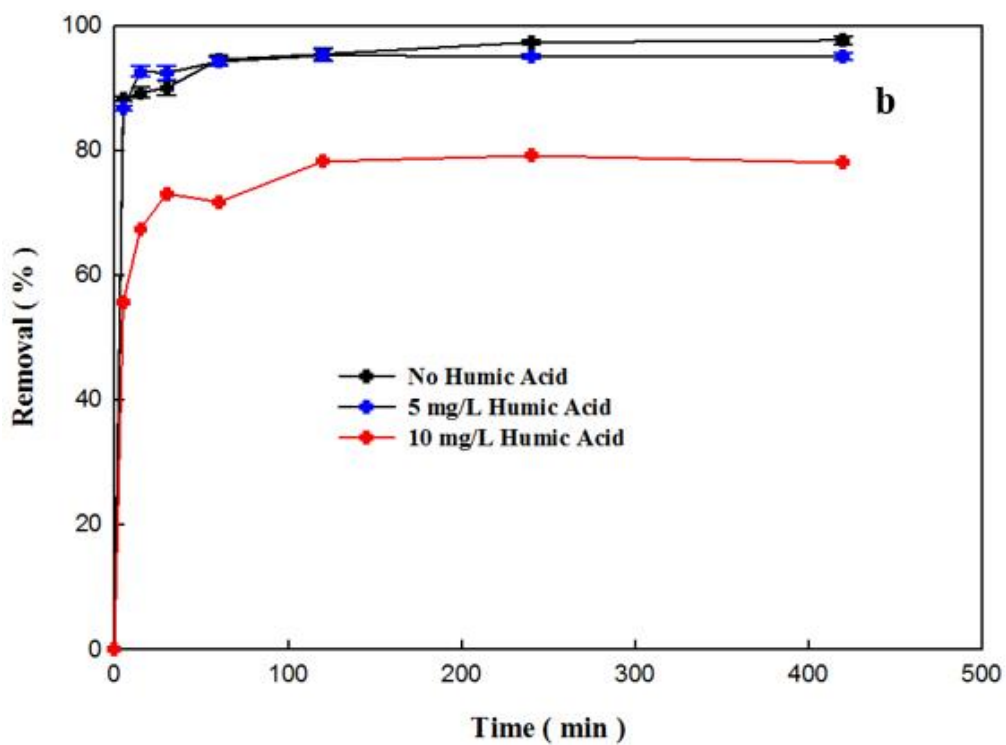
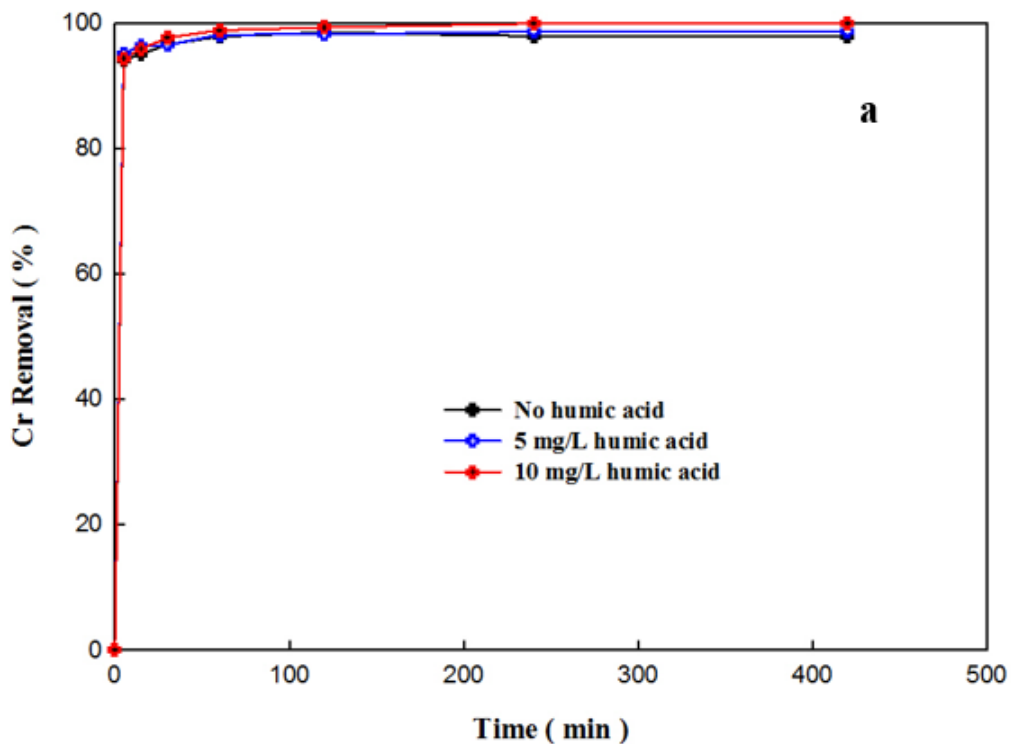


Figure 10 Effect of humic acid on C(VI) adsorption. (a) bare Fe-Mn. (b) starch stabilized Fe-Mn.

Initial Cr(VI) = 5 mg/L, nanoparticle = 0.27 g/L (Fe = 0.2 g/L, Mn = 0.07 g/L).

### 3.7 Cr(VI) immobilization in soil: column tests

Fig. 11. Presents the breakthrough curve of starch stabilized Fe-Mn nanoparticles, at flow rate of 0.15 mL/min, the full breakthrough occurred at about 4 pore volumes, nearly 20% particles were retained on column.

Starch stabilized Fe-Mn nanoparticles used to treat the Cr(VI) landed soil in the same column, for comparison, DI was applied with the same process. Fig. 12 shows the result of immobilization test. Calculated by mass balance, DI water remove 79% of total Cr(VI) from soil, while nanoparticles eluted 67% of Cr(VI). In nanoparticle elution, 18% of Cr(VI) is soluble, 82% of Cr(VI) was adsorbed on nanoparticles. Compare with DI water elution, the soluble Cr(VI) was reduced by 85%.

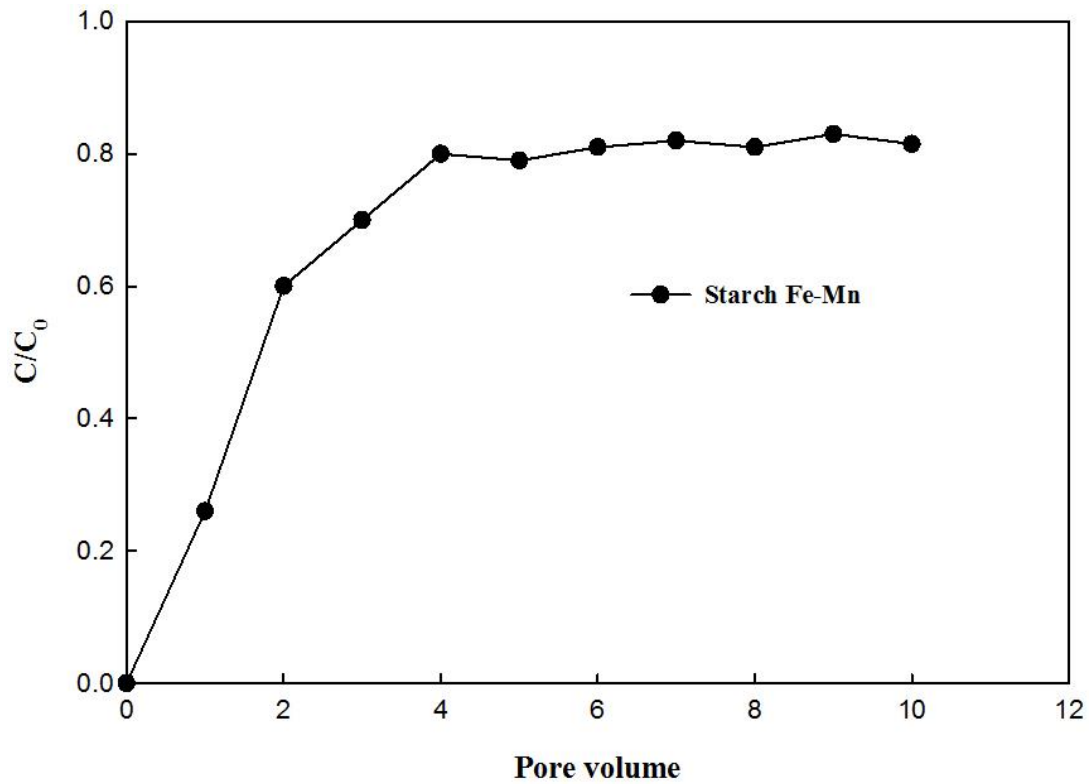


Figure 11 Breakthrough curve of starch stabilized Fe-Mn nanoparticles through a sandy loam soil bed. Nanoparticle = 0.27 g/L (Fe = 0.2 g/L, Mn = 0.07 g/L), starch = 0.19 wt. %, pH = 6.0. EBCT = 71 min, flow velocity = 0.15 mL/min

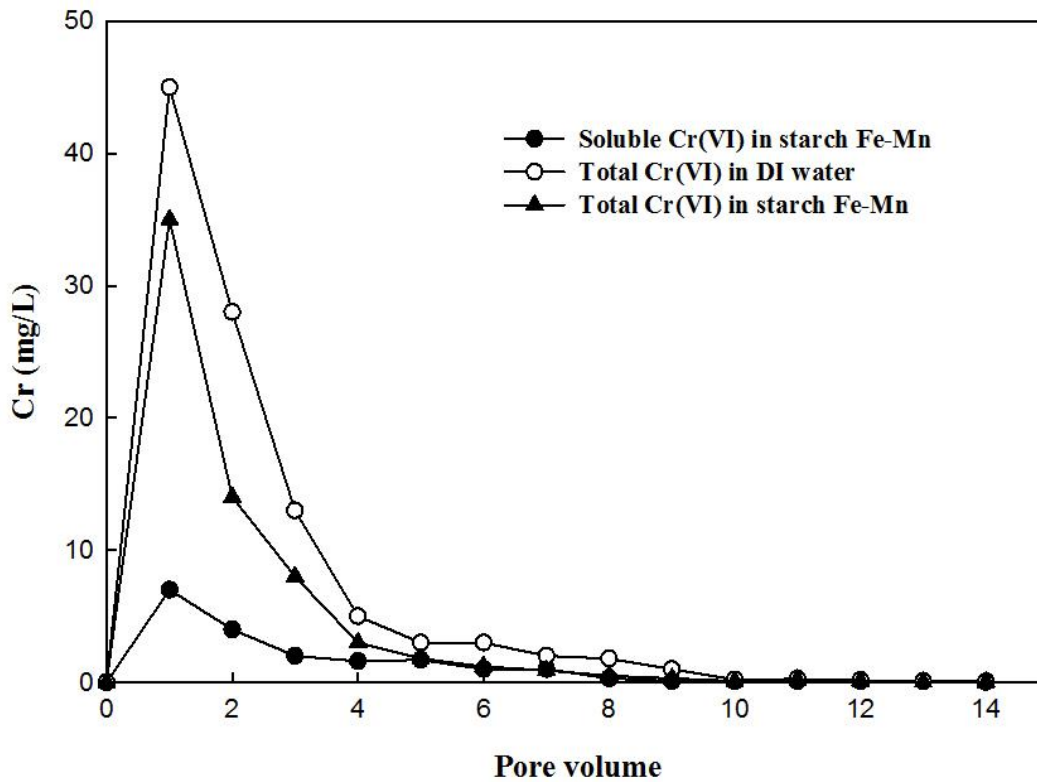
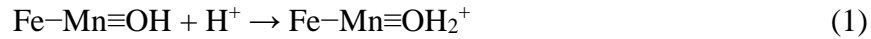


Figure 12 Cr(VI) concentration profiles in elution using DI water and starch stabilized Fe-Mn nanoparticle. Initial condition: Cr spiked soil = 87 mg/kg, nanoparticle = 0.27 g/L (Fe = 0.2 g/L, Mn = 0.07 g/L), starch = 0.19 wt. %, pH = 6.0-6.3. EBCT = 71 min, flow velocity = 0.15 mL/min.

### 3.5 Conclusions

The main conclusions were summarized as follows:

- Base on FTIR and XPS analysis, the adsorption of Cr(VI) on Fe-Mn processes as Eqns 1-4, the electrostatic attraction is the most important driving force. No reduction reaction of Cr(VI) during adsorption.



- The starch stabilized Fe-Mn offer a comparable adsorption capacity to bare particle while removal of chromate was restrained by CMC stabilizer due to its negative charge. The Langmuir adsorption capacity of bare, starch and CMC stabilized nanoparticle were 59 mg/g, 54 mg/g, and 2 mg/g, respectively.
- The adsorption of chromate is highly sensitive to pH. The optimal working pH of this particle is 5 to 6.
- The starch stabilized Fe-Mn can offer high selectivity and removal efficiency in the presence of competing ions sulfate and phosphate. The removal efficiency drop is negligible when  $\text{HA} < 5\text{mg/L}$ .
- Starch stabilizer offered a slight lower Cr(VI) removal efficiency compare to bare particles. But the introduction of stabilizer enable the particle to be deliverable in soil. Additional, removal efficiency of bare particle was reduced to 12% and 5% by 0.1mM and 1mM of phosphate, while the value for starch stabilized Fe-Mn

was 73 % and 34%, respectively. The starch coating offer greater selectivity of Fe-Mn nanoparticles toward Cr(VI).

- Column breakthrough test indicated that about 20% of starch stabilized Fe-Mn nanoparticles were retained in soil after breakthrough, indicated the potential of delivery into soil.
- Immobilization test indicated that after 15 PVs, the soluble Cr(VI) in elution was reduced by 85%.

## References

- Aravindhnan, R. M. (2004). Bioaccumulation of chromium from tannary wastewater: an approach for chrome recovery and reuse. *Environ. Sci. Technol.*, *38*, 300-306.
- Baral A, E. R. (2002). Chromium-based regulations and greening in metal finishing industries in the USA. *Environmental Science Policy*, *5*, 121-133.
- Barnhart, J. (1997). Occurrences, Uses, and Properties of Chromium. *Regulatory toxicology and pharmacology*, *26*, S3-S7.
- Bessbousse, H. (2008). Removal of heavy metal ions from aqueous solutions by filtration with a novel complexing membrane containing poly(ethyleneimine) in a poly(vinyl alcohol) matrix. *Journal of membrane Science*, *307*(2), 249-259.
- Biggs, S. (2006). *Encyclopedia of surface and colloid science* (Vol. 7). New York: Taylor and Francis.
- Byungryul An, D. Z. (2012). Immobilization of As(III) in soil and groundwater using a new class of polysaccharide stabilized Fe-Mn oxide nanoparticles. *Journal of Hazardous Materials*, 332-341.
- C. Su, D. S. (2000). Selenate and selenite sorption on iron oxides: an infrared and electrophoretic study. *Soil Sci. Soc. AM.*, *64*, 101-111.
- Chad P. Johnston, M. C. (2014). Mechanisms of chromate adsorption on hematite. *Geochimica et Cosmochimica Acta*, *138*, 146-157.
- Changyan Gao, J. Q. (2012). low-cost synthesis of flowerlike  $\alpha$ -Fe<sub>2</sub>O<sub>3</sub> nanostructures for heavy metal ion removal: adsorption property and mechanism. *Langmuir*, *38*, 4573-4579.
- Dantas, T. N. (2001). Removal of chromium from aqueous solutions by diatomite treated with microemulsion. *Water Res.*, *35*, 2219-2224.
- Fang J, G. D. (2007). Cr(VI) removal from aqueous solution by activated carbon coated with quaternized poly(4-vinylpyridine). *Environmental science & technology*, *41*(13), 4748-4753.
- Gaosheng Zhang, J. Q. (2007). Preparation and evaluation of a novel Fe-Mn binary oxide adsorbent for effective arsenite removal. *Water Research*, 1921-1928.
- Haisa, T. H. (1993). Chemical and spectroscopic evidence for specific adsorption of chromate on hydrous iron oxide. *Chemosphere*, 1897-1904.
- Jiang Wj, P. M. (2013). Chromium(VI) removal by maghemite nanoparticles. *Chem Eng*, 527-533.
- Jing Hu, G. C. (2005). Removal and recovery of Cr(VI) from wastewater by maghemite nanoparticles. *water research*, *39*, 4528-4536.

- Kizil, R., I rudayaraj, J., & Seetharaman, K. (2002). Characterization of irradiated starches by using FT-Raman and FTIR spectroscopy. *J. Agr. Food Chem.*, 50(14), 3912-3918.
- Kontos A I, L. V. (2009). Self- organized anodic TiO<sub>2</sub> nanotube arrays functionalized by iron oxide nanoparticle. *Chemistry of materials*, 21(4), 662-672.
- Kurniawan, T. A. (2006). Physico-chemical treatment techniques for wastewater laden with heavy metals. *Chemical Engineering Journal*, 118(1-2), 83-98.
- Lei Z, Z. J. (2012). Ultrathin MnO<sub>2</sub> nanofibers grown on graphitic carbon spheres as high-performance asymmetric supercapacitor electrodes. *Journal of materials Chemistry*, 22(1), 153-160.
- Liang, Q. Z. (2012). Effects of stabilizers and water chemistry on arsenate sorption by polysaccharide-stabilized magnetite nanoparticles. *Ind. Eng. Chem. Res.*, 51, 2407-2418.
- M. Nameni, M. R. (2008). Adsorption of hexavalent chromium from aqueous solutions. *International Journal of Environmental Science & Technology*, 161-168.
- Marinin, D. (2000). Studies of sorbent/ion-exchange materials for the removal of radioactive strontium from liquid radioactive waste and high hardness groundwater. *Waste Management*, 20, 545-553.
- Mojdeh Owlad, M. K. (2009). Removal of Hexavalent Chromium-Contaminated Water and Wastewater: A Review. *Water Air Soil Pollut*, 200, 59-77.
- Peterson M, B. G. (1996). Direct XAFS evidence for heterogenous redox reaction at the aqueous chromium/magnetite interface. *Colloids Surf A*, 107, 77-83.
- R. K. Tandon, P. T. (1983). Effect of pH on Chromium(VI) species in solution. *Analytical data*, 227-228.
- Shaima S. Hamdan, M. H.-N. (2014). Characterization of the removal of chromium(VI) from groundwater by electrocoagulation. *Journal of Industrial and Engineering Chemistry*, 2775-2781.
- Sphsite, G. (1989). *The chemistry of soils*. New York: Press.
- W.F. Tan, S. L. (2008). Determination of the point of zero charge of manganese oxides with different methods including an improved salt titration method. *Soil Sci.*, 173, 277-286.
- Wangwang Tang, G. Z. (2014). Impact of humic/fulvic acid on the removal of heavy metals from aqueous solutions using nanoparticles: A review. *Science of the total Environment*, 1014-1027.
- Weng, C. W. (1997). adsorption of Cr(VI) onto TiO<sub>2</sub> from dilute aqueous solutions. *Water Sci. Technol.*, 35, 55-62.
- Wenjun Jiang, M. P. (2013). Chromium(VI) removal by maghemite nanoparticles. *Chemical engineering journal*, 222, 527-533.
- Xiong L, C. C. (2011). Adsorption of Ph(II) and Cd(II) from aqueous solutions using titanate nanotubes prepared via hydrothermal method. *Journal of hazardous materials*, 189(3), 741-748.
- Yang Gao, J. X. (2011). Chromium Contamination Accident in China: Viewing Environment Policy of China. *Environmental Science & Technology*, 45, 8605-8606.

Zhao, D. Y. (2010). Effect of environmental conditions on Pb(II) adsorption on  $\beta$ -MnO<sub>2</sub>. *Chem. Eng.*, 164, 49-55.